TECHNICAL REPORT ARCCB-TR-88027

FATIGUE - FRACTURE PROPERTIES OF A SEMI-AUSTENITIC PRECIPITATION HARDENING STAINLESS STEEL

R. FARRARA

JUNE 1988

US ARMY ARMAMENT RESEARCH, DEVELOPMENT AND ENGINEERING CENTER
CLOSE COMBAT ARMAMENTS CENTER
BENÉT LABORATORIES
WATERVLIET, N.Y. 12189-4050

APPROVED FOR PUBLIC RELEASE; DISTRIBUTION UNLIMITED

DISCLAIMER

The findings in this report are not to be construed as an official Department of the Army position unless so designated by other authorized documents.

The use of trade name(s) and/or manufacturer(s) does not constitute an official indorsement or approval.

DESTRUCTION NOTICE

For classified documents, follow the procedures in DoD 5200.22-M, Industrial Security Manual, Section II-19 or DoD 5200.1-R, Information Security Program Regulation, Chapter IX.

For unclassified, limited documents, destroy by any method that will prevent disclosure of contents or reconstruction of the document.

For unclassified, unlimited documents, destroy when the report is no longer needed. Do not return it to the originator.

SECURITY CLASSIFICATION OF THIS PAGE (When Data Entered)

REPORT DOCUMENTATION PAGE

READ INSTRUCTIONS BEFORE COMPLETING FORM

1. REPORT NUMBER ARCCB-TR-88027	2. GOVT ACCESSION NO.	3. RECIPIENT'S CATALOG NUMBER
4. TITLE (and Subtitle) FATIGUE - FRACTURE PROPERTIES OF A SEMI-AUSTENITIC PRECIPITATION HARDENING STAINLESS STEEL		5. TYPE OF REPORT & PERIOD COVERED Final 6. PERFORMING ORG. REPORT NUMBER
7. AUTHOR(s) R. Farrara		8. CONTRACT OR GRANT NUMBER(s)
9. PERFORMING ORGANIZATION NAME AND ADDRESS US Army ARDEC Benet Laboratories, SMCAR-CCB-TL Watervliet, NY 12189-4050		10. PROGRAM ELEMENT, PROJECT, TASK AREA & WORK UNIT NUMBERS AMCMS No. 6126.23.1BL0.0AR PRON No. 1A72RZPJNMSC
11. CONTROLLING OFFICE NAME AND ADDRESS US Army ARDEC Close Combat Armaments Center Picatinny Arsenal, NJ 07806-5000		12. REPORT DATE June 1988 13. NUMBER OF PAGES 26
14. MONITORING AGENCY NAME & ADDRESS(if different from Controlling Office)		15. SECURITY CLASS. (of this report) UNCLASSIFIED 15a. DECLASSIFICATION/DOWNGRADING SCHEDULE

16. DISTRIBUTION STATEMENT (of this Report)

Approved for public release; distribution unlimited.

17. DISTRIBUTION STATEMENT (of the abstract entered in Block 20, if different from Report)

18. SUPPLEMENTARY NOTES

Published as Technical Report No. MRL-R-1041, Materials Research Laboratories, Victoria, Australia, February 1987.

19. KEY WORDS (Continue on reverse side if necessary and identify by block number)

Stainless Steels	Crack Propagation
Precipitation Hardening Steels	Fatigue
105-mm Light Gun	Gun Carriages
Fracture Toughness	

20. ABSTRACT (Continue on reverse side if necessary and identify by block number)

Fatigue and fracture toughness properties were determined for STA 60 precipitation hardening stainless steel used in the structure of the 105-mm Light Gun. Fatigue properties (S-N crack for initiation and da/dN versus ΔK crack growth rate) and fracture toughness (J_{IC}) were measured on both parent sheet and welded joints for a range of heat treatments including fully re-heat treated and peak aged (450°C), overaged as in production (530°C), and as-welded joints not re-heat treated.

(CONT'D ON REVERSE)

DD FORM 1 JAN 73 1473 EDITION OF 1 NOV 65 IS OBSOLETE

UNCLASSIFIED

SECURITY CLASSIFICATION OF THIS PAGE (When Data Entered)

20. ABSTRACT (CONT'D)

The material was found to be notch sensitive. Fatigue crack growth was much faster, and fracture toughness much lower, in the longitudinal (rolling) direction of the sheet because of the presence of nonmetallic stringers in the microstructure. Overaging had little effect on fatigue properties compared with peak aging, but did achieve a significant improvement in fracture toughness. Weld metal was more resistant to fatigue crack initiation than parent sheet, but welds not re-heat treated were drastically limited in all three properties because the weld heat-affected zones remained in the soft condition.

C O N T E N T S

TABLES

LIST OF ILLUSTRATIONS

FATIGUE - FRACTURE PROPERTIES OF A SEMI-AUSTENITIC PH STAINLESS STEEL

1. INTRODUCTION

The UK designed 105-mm Light Gun (L118/L119) incorporates a light weight carriage fabricated from high strength, precipitation hardening (PH) stainless steel sheet. The high, cyclic stresses applied during firing may generate fatigue cracks in both the parent metal and near welded joints.

The objectives of this report are to

(a) provide the standard quantitative fatigue and fracture properties (crack propagation rate and fracture toughness) of the parent material which can be used to predict fatigue life and establish defect limitations;

(b) determine if the resistance to fatigue cracking of a welded joint with the weld bead machined flush to the parent material is greater or less than that of the parent material;

(c) to compare the fatigue and fracture properties that result from ageing at 530°C (temperature selected for the weldment) and 450°C. The lower age temperature has been reported to provide higher strength hence potentially better resistance to fatigue cracking;

(d) to determine the degradation in fatigue resistance that would occur in a repair welded joint that is not heat treated after welding.

2. MATERIAL

The parent material is a semi-austenitic PH stainless steel that conforms to British Standard 95-15, and is designated STA60. It is austenitic at room temperature after a solution treatment at 1050°C and air cooling; hence it can be severely cold formed to produce sheet and the sheet metal can be extensively shaped in a relatively soft condition without risk of cracking, giving potentially a large advantage in manufacturing. It is readily weldable (carbon content less than 0.1%) and distortion or cracking does not occur from heat treatment. This material is understood to have been selected on the basis of fatigue performance of welded specimens. The composition is listed in Table 1 and the mechanical properties are listed in Table 2.

The weldments are produced by the tungsten inert gas (TIG) process with 1.2 mm diameter filler wire. The welding wire is a martensitic PH stainless steel that conforms to the British Standard 95-14 (STA59). This material is not austenitic at room temperature; however it can be cold drawn to produce wire by ageing the martensite at 620°C prior to cold working. The postulated reason for using it as filler metal is that since the chromium is approximately 2% less than the parent material, the quantity of delta ferrite in the weld nugget is reduced, which improves the mechanical properties of a weldment. The composition is listed in Table 1 and the mechanical properties of welded specimens are listed in Table 2.

2.1 Heat Treatment

The four major stages are as follows:

S: Solution treatment at 1050°C (5 minutes) followed by air cooling. This is the as-supplied condition.

C: Conditioning at 750°C (2 hours) and air cool. (Also termed "trigger anneal"). Carbon is rejected from solution which raises the M_s and M_f temperatures thereby allowing the destabilized austenite to transform to martensite by cooling to slightly below room temperature.

SC: Sub-Zero Cool to below -5°C (2 hours). This step assures complete transformation to martensite.

PH: Precipitation harden, also called ageing, by heating to a desired temperature for 2 hours. The ageing temperature specified for the production units is 530°C, which is in fact an overage, the peak ageing temperature being 450°C for this material. The convention adopted in this report is that the 530°C treatment is termed overaging and the 450°C treatment, normal ageing. Hardening and strengthening occurs during ageing by precipitation of fine intermetallics, carbides and phosphides.

The heat treatment procedure for the actual weldment is to apply the C & SC steps to the components prior to welding. This avoids dimensional changes after welding, because the volumetric change occurs during transformation of austenite to martensite. After welding a complete heat treatment is applied (C, SC, and PH) to eliminate the heat-affected zones and to strengthen the material.

The heat treatment procedure for the repair weld condition was to apply a complete heat treatment (C, SC, and PH) to the material prior to welding, with no further heat treatment after welding.

3. EXPERIMENTAL

3.1 Fatigue and Fracture Toughness Testing

The following tests were carried out:

(a) **Constant Amplitude Axial Fatigue** (S-N per ASTM E-466). This is basically a test used for comparing the resistance to crack initiation of different material conditions. It was used to compare the parent material with a heat treated weldment and with a repair weld condition. Also it was used to compare the overage treatment with the normal age treatment.

(b) **Constant Load Amplitude Fatigue Crack Growth Rates** (da/dN vs ΔK per ASTM E-647). This test provides the constants, C and m, needed for the crack propagation rate equation (Paris Law) which is $da/dN = C\Delta K^m$. It was conducted on parent material with the cracking direction both parallel and transverse to the rolling direction. Also both ageing temperatures were evaluated. Tests were done in the regime above 10^{-8} m/cycle.

(c) **J_{Ic}, A Measure of Fracture Toughness** ((J_{Ic}) per ASTM E-813). This test provides an estimate of the stress intensity (K_{Jc}) required to initiate extension of a crack in a specimen subject to a static load. Also it provides an estimate of how much resistance the material has to rapid, unstable crack growth. It is used instead of the K_{Ic} test because the material is so thin that the required unstable crack growth and plane-strain stress conditions cannot be met.

3.2 Specimens

Test specimens were prepared for each of the above tests, as follows:

(a) **S-N specimens**. Flat, rectangular, tensile specimens with a reduced cross-section as shown in Fig. 1a were removed from 3.2 mm sheet. The longitudinal axis of the specimen was transverse to the rolling direction which would accentuate a potential anisotropic effect. The surface finish requirement along the sides of the test section mandated a machining operation. Twenty-four (24) parent material specimens (12 overaged, 12 normal aged), twenty-four (24) weld plus heat treated specimens (12 overaged, 12 normal aged), and twelve (12) repair weld specimens (complete heat treatment prior to welding - no heat treatment after welding) were manufactured.

(b) **da/dN vs** ΔK . Compact tension (CT) specimens were removed from 6 mm thick plates of parent material and machined to the MRL design shown in Fig. 2. Eight (8) specimens were manufactured from heat treated plates - four (4) were overaged and four (4) were normal aged. Test results from cracks growing both transverse and parallel to the rolling direction were desired hence two (2) specimens for each direction were taken for each ageing condition.

(c) $\mathbf{J_{Ic}}$ **Fracture Toughness**. The above CT specimens were also used to measure J_{Ic} after the da/dN tests were completed. This design features a third non-loading hole that is easy to machine and generates integral knife edges for a clip gage to measure load-line deflection.

3.3 Testing Procedures

(a) **S-N tests**. All fatigue specimens were loaded in tension with a 500 kN MTS servohydraulic machine under load control (accuracy of 1%). The ends of the specimens were clamped by serrated grips and the alignment was maintained by a series of pin joints. Since load control is used failure will occur soon after a crack is initiated hence the number of cycles to failure represents closely the number of cycles to initiate a crack. In order to avoid cracking at the wrong location the width of the test section was at first decreased from 20 mm to 18 mm and the hole was reamed to improve the surface finish. A few of these remachined specimens failed in the test cross-section but several specimens continued to fail at the hole.* It was therefore decided to drastically reduce the test cross-section to 12 mm x 2 mm as shown in Fig. 1(b) on all of the remaining specimens (two parent material, twenty-four weld plus heat treat, twelve repair weld). All of these specimens (Fig. 1(b)) failed in the test cross-section as required.

(b) **da/dN vs** ΔK **tests**. These tests were conducted in a 250 kN, MTS servohydraulic machine under load control (accuracy of 1%). A clevis-pin assembly with teflon washers for centering the specimen between the clevis was used for loading the specimens. The crack length was measured on both sides of the specimen (average value used for calculations) using 4X travelling microscopes with reference marks scribed 1 mm apart on the specimens as aids. The number of elapsed cycles (multiplication factor of 10) was recorded and the crack length was measured accurately after an approximate change in crack length of 1 mm.

(c) $\mathbf{J_{Ic}}$ **Test**. The CT specimens were then loaded under displacement control with the 250 kN MTS machine and clevis-pin assembly used for the da/dN test. The tests were computer controlled and the 10% unload-compliance measurement technique was used to calculate the change in the physical crack length (Δa_p).

---

* Arising from difficulty in maintaining sufficient clamping force.

The precrack for the J test was the fatigue crack generated from the da/dN test. The maximum load applied during the da/dN test was 7 kN which is less than the 0.4 P_L requirement of E813, however the final $\Delta K/E$ value was approximately 0.01 $mm^{1/2}$ which is obviously greater than the requirement of 0.005 $mm^{1/2}$ or less. Too high a ΔK during precracking can affect the fracture toughness results and may cause the test value to be slightly higher than normal [1].

The J vs Δa_p data points, the blunting line, the 0.15 mm and 1.5 mm offset lines, and the linear regression line were plotted by computer. The standard equation outlined in ASTM E813 was used by the computer to calculate J.

4. RESULTS AND DISCUSSION

4.1 S-N Fatigue Tests

The fatigue testing of parent material specimens made to Fig. 1(a) resulted in failures at one of the holes nearest to the test cross-section. It should be noted that the dimensions shown in Fig. 1(a) (20 mm x 3 mm) were used successfully by Clark [2] in fatigue testing the subject material to compare the effects of the free-edge surfaces produced by laser cutting versus machining.

An important result from the initial testing is that crack initiation of this material is very dependent upon, and sensitive to surface roughness. Surface roughness of the machined edge along the test section for the initial specimens (Fig. 1(a)) was 3.2 µm maximum (actual values were 1.5 to 2.0 µm) whereas measured values of a sample machined specimen used by Clark [2] were 3.25 µm on one side and in excess of 10 µm on the other side. The maximum value specified for specimens made to Fig. 1(b) is 0.8 µm and measured values were a maximum of 0.5 µm.

The S-N data are listed in Table 3 and a $\log_{10}$-$\log_{10}$ plot of S-N is shown in Fig. 3. There are only two linear regression lines on Fig. 3 - repair weld, weld with normal age and overage combined since the difference resulting from the two ageing temperatures was insignificant. The two parent metal-overaged specimens were included with the welded - and - overaged specimens because all the weld heat-treated specimens failed in the parent material away from the weld. This indicates that the weld metal is more resistant to crack initiation than the parent metal and effectively all of the data from the welded - and - heat-treated specimens represents the fatigue resistance of the parent material. It should be noted that the welds were machined smooth and blended with the parent material. If the weld bead were left "as welded" the failure location probably would have been at the stress concentration created at the weld bead - parent material intersection (i.e. the weld toe) and the number of cycles to failure probably would have been less than realized with the specimens tested for this report. The failure location for all of the **repair welded specimens** was in the heat-affected zone next to the weld metal. Yielding was visible at both heat-affected areas after the first cycle at all of the stress levels (lowest of 600 MPa) which is as expected since the yield strength shown in Table 2 is less than 600 MPa (523 MPa).

Plotting the data on a log-log scales reveals a linear correlation between log S and log N which allows the stress to be a function of life in the form $S = CN^{-m}$ where C is $10^{(Y\ \mathrm{intercept})}$ and m is the slope. The equations are listed on Fig. 3 and it is suggested that they could be used as an engineering tool to estimate the number of cycles at a specific cyclic tensile stress to initiate a crack providing the surface roughness was 0.8 μm maximum. Using the equation for parent metal $S = 2.857 \times 10^{3}\ N^{-.110}$ the stress required to initiate failure at 10^{6} cycles (endurance limit) is 625 MPa which is approximately 60% of the material's yield strength. It is the author's opinion that this is superior to the typical high strength steel especially considering that the orientation of the specimen axis was transverse to the rolling direction.

4.2 da/dN vs ΔK Test

The data from all of the eight specimens (two specimens per direction for each ageing temperature) was plotted with the result that in all cases a smooth curve could be drawn through the points. The da/dN values, calculated by the secant method versus N values were plotted on a $\log_{10}$ - $\log_{10}$ scale shown in Figures 4 and 5. A least square-linear line through the data allows the calculation of the constants C and m for the standard crack growth law - $da/dN = C\Delta K^{m}$. A few of the data points obtained for the longitudinal specimens were not used for the calculations as shown in Fig. 4. The reason these points were excluded is that these ΔK values were approaching the K_c value (rapid unstable crack growth) which was determined by the fracture toughness (J_{Ic}) testing. The comparisons are overage-longitudinal vs normal age-longitudinal on Fig. 4 and overage-transverse vs normal age-transverse on Fig. 5. Table 4 provides a summary of the pertinent data.

The data shows that the two ageing treatments result in approximately the same crack propagation rate however the rate in the longitudinal direction (i.e. along the rolling direction) is significantly greater than the transverse direction. During precracking of the longitudinal specimen it became obvious there was a problem with growing a crack parallel to the rolling direction because the crack did not grow uniformly, i.e. the crack grew much more on one side than the other side of the specimen. In order to force uniform growth the specimen was shifted off the centerline of the load cell by using different thicknesses of teflon washers between the clevis and the specimen. This allowed the short crack to "catch-up" with the long crack and thereafter the crack grew uniformly, i.e. both sides of the specimen had approximately the same crack growth and length.

4.3 J_{Ic} Fracture Toughness Test

The J_{Ic} test data are listed in Table 5 and J vs Δa_p plots are shown on Fig. 6 for the overaged material and on Fig. 7 for the normal aged material.

The data in Table 5 allows a comparison of the initial crack length normalized by specimen width (a_o/w) and the final crack extension (Δa_f) that was obtained from the 10% unload-compliance technique to the physically measured values obtained after heat tinting and fracturing. The comparison reveals that a_o/w calculated by the compliance technique was for all specimens slightly less than the physically measured value however the difference is not enough to be considered important. Nevertheless, the Δa_f values obtained by the compliance technique are considerably less than the physically measured values because of crack tunnelling. The difference between the two values exceeded the ± 15% limitation specified in E813 hence the values reported for J_{Ic} are not strictly valid in accordance with ASTM E813.

The data reveals the ageing temperature is important and, as expected from the da/dN data, the direction of cracking is important. The overage temperature resulted in significantly better fracture toughness than the normal age temperature. Comparing the OT specimens to the NT specimens reveals large differences in J_{Ic} and $\Delta J/\Delta a_p$ slope values and comparing the OL specimens to the NL specimens reveals much smaller differences in the value of J_{Ic} values but large differences in the slope ($\Delta J/\Delta a_p$) values. It is obvious by comparing the L direction to the T direction that there is a large effect of material anisotropy which would lead to problems in service where fatigue crack growth rate is the life-limiting factor.

The J_{Ic} and slope ($\Delta J/\Delta a_p$) data can be used to obtain an approximate value of critical crack depth (a_c), i.e. the depth at which unstable crack growth occurs. The J_{Ic} value can be converted to a K_{Jc} value because it is the value at which crack extension is initiated and stress-strain conditions are essentially linear-elastic. The a_c value is calculated from the stress intensity equation $K_{Jc} = \sigma_{nominal} \sqrt{a_c}.Y$ where Y is the K calibration value. Y is usually a polynomial function of a/w and is available for many specimen configuration-loading arrangements. In order to obtain a feel for a_c values assume the component could be approximated by a semi-infinite plate that was subject to a nominal tensile stress with a crack extended in from one side. Y for this configuration is approximately 2, i.e. $K = 1.12\ \sigma_n \sqrt{\pi a} \approx 2\ \sigma_n \sqrt{a}$. The following tabulation is for $\sigma_{nominal}$ vs a_c for the longitudinal and transverse direction, for material in the overaged condition. Approximate values of K_{Jc} are estimated from Table 5 : 60 MPa $\sqrt{m}$ for OL and 150 MPa $\sqrt{m}$ for OT material.

σ_n (MPa)	Longitudinal a_c(mm)	Transverse a_c (mm)
100	90	560
500	3.6	22.4
800	1.4	8.8

Obviously the high toughness associated with the transverse direction results in large values of a_c, especially if the nominal stress is low. Also it is important to realise that the value of K_{Jc} calculated for the transverse direction is conservative compared to the value used for the longitudinal direction. The reason for this is that K_{Jc} is the calculated stress intensity that is required to start crack extension. The K required to cause rapid unstable crack extension (K_c) is certainly greater than K_{Jc} and the difference can be correlated to the $\Delta J/\Delta a_p$ slope which is a measure of the resistance to crack extension. Since the $\Delta J/\Delta a_p$ slope for the transverse direction is much greater than for the longitudinal direction the amount that K_c exceeds K_{Jc} for the transverse direction is much greater than for the longitudinal direction.

4.4 Directionality in Properties

Since the toughness and crack propagation rate values for the rolling direction (longitudinal) are much worse than for the transverse direction, a scanning electron microscope (SEM) examination was conducted on the fracture surface created during fatigue cracking. Numerous manganese sulphide stringers were observed which can be seen in Fig. 8. Stringers offer an easy path for a crack propagating along their length however they do not affect, to any large degree, the resistance to a crack propagating transverse to the rolling direction.

It was immediately assumed, erroneously, that the stringers were caused by too high a sulphur content. Accurate measurement revealed that the sulphur content is actually quite low (0.008% or less), and obviously reducing the sulphur content further would not be the approach to pursue. If manganese sulphides, which are malleable, exist in the original ingot they will be stretched to form stringers due to the severe area reductions that occur during rolling to plate or sheet. If the steel melt were to be refined by a calcium treatment which results in non-malleable particles, stringers would not be generated during rolling and the anisotropy problem should be drastically reduced.

In practical applications of this steel, the absolute difference in total fatigue life for a crack initiated parallel versus transverse to the rolling direction may not be nearly as large as indicated by crack propagation rates because the majority of the total life is spent initiating the crack. The major concern from the directionality condition is in fact the resistance to rapid-unstable fracture. The example for calculating critical crack depth reveals that the value of a_c may be extremely small, depending upon the applied stress level, for cracks parallel to the rolling direction. Also since the slope of the toughness-crack extension data ($\Delta J/\Delta a_p$) is small for the longitudinal direction the value calculated for a_c is not very conservative, i.e. rapid-unstable growth will occur at approximately the theoretical value which is based on linear-elastic stress intensity (K_{JC}) fracture theory.

5. CONCLUSIONS

5.1 **Fatigue Crack Initiation** (S-N Tests)

(a) The material is notch sensitive hence surface roughness has a dramatic effect on the crack initiation phase of fatigue. The resistance to crack initiation is excellent provided that stress concentrations caused by surface roughness and weld toes are removed.

(b) The weld filler material is more resistant to crack initiation than the parent material. This is probably because there are fewer inclusions (manganese sulphide stringers) and therein fewer weak spots in the weld metal.

(c) Ageing at a lower temperature, 450°C as against 530°C, increases yield strength but does **NOT** improve the resistance to crack initiation. This aspect correlates with notch sensitivity, in that when material is notch sensitive, increasing the yield strength via heat treatment will not usually improve resistance to crack initiation.

(d) Repair welding without heat treatment after welding will cause a drastic reduction in fatigue life and strength due to the low strength heat-affected zone, which remains in the austenitic condition.

5.2 **Fatigue Crack Growth Rate** (da/dN vs ΔK Test)

(a) The crack growth rate of the parent material for the longitudinal direction (parallel to rolling direction) is much greater than for the transverse direction. Directionality is caused by manganese sulphides which are elongated by the severe reduction that occurs during the rolling of plate and sheet.

(b) The overage temperature (530°C) results in a slightly lower crack growth rate than the normal age temperature (450°C).

5.3 **Fracture Toughness Tests** (J_{IC} Tests)

(a) The fracture toughness, J_{IC}, and the resistance to rapid-unstable cracking measured by the $\Delta J/\Delta a_p$ slope are drastically affected by directionality. Both values are much lower for a crack orientated parallel to the rolling direction than for a crack orientated perpendicular to the rolling direction.

(b) The fracture toughness is also affected by the ageing temperature. The toughness is significantly higher for the overage (530·C) temperature, which is the temperature employed in the production of gun components.

5.4 General Conclusions

(a) The resistance to crack initiation is excellent provided that stress concentrations (rough surfaces, weld toe) are removed. However once a crack is initiated it may propagate rapidly and only to shallow depth before final rapid fracture occurs.

(b) Directionality, caused by manganese sulphide stringers, drastically reduces the resistance to crack propagation and the critical crack depth for a crack orientated parallel to the rolling direction.

6. RECOMMENDATIONS

(a) Stress concentrations should be minimized as much as possible by blending weld beads smooth with the parent material and by requiring a reasonable surface roughness (2.5 μm max) on free-edge surfaces. A large percentage of the fatigue life is the crack initiation phase hence care in prevention of cracks will be worth the effort.

(b) The NDT defect criterion for both new construction and field useage has to be restrictive because of the low fracture toughness properties and high propagation rate for the longitudinal direction. Since the major portion of the total fatigue life is the cycles needed for initiating and propagating a shallow crack, if a crack-like defect is allowed to exist in new construction, the fatigue life will be dramatically reduced. The critical crack depth value is small due to the low toughness properties hence areas that are known from experience to be susceptible to cracking (high stressed areas) should be inspected often. Any discovered cracks should be removed if practical or repairs accomplished, otherwise rapid unstable crack growth could occur after a relatively small number of additional cycles.

The above statements are made on the assumption that (a) the principal tensile stress direction is perpendicular to the rolling direction of the plate hence a crack that initiates will be propagating parallel to the rolling direction and (b) a surface containing a crack will continue to sustain the high load that caused the crack to initiate, i.e., the loading is not transferred to an uncracked component thereby drastically reducing the stress applied to the cracked component.

(c) The specification requirements used for purchasing the parent material should be upgraded, for example by calcium modification of the steel, to eliminate the manganese sulphide stringers thereby raising toughness and lowering crack propagation rates.

The recommended methods are to (1) specify that the maximum sulphur be reduced from 0.025 to 0.010 wt% (2) specify that a calcium treatment process should be used during the melting process in order to tie up the sulphur as small, spherical shaped, calcium sulphide particles that are not malleable, and (3) a cleanliness specification such as AMS 2300 should be required.

7. ACKNOWLEDGEMENTS

The author is appreciative of Dr David Saunders for his advice and for providing all of the work input-output with the computers. I am also appreciative of Mr Tom Rea for his advice and guidance and of Mr Ian Burch for conducting the J Integral Tests.

The work was undertaken while the author was on a scientist exchange from Benet Weapons Laboratory, Watervliet Arsenal, Watervliet, N.Y., USA.

8. REFERENCES

[1] Clark, G. Fracture Toughness of Fatigue Damaged Steel Specimens, Report MRL-R-749, Materials Research Laboratories, Melbourne, Australia (1979).

[2] Clark, G. Fatigue Performance of Laser Cut and Conventionally Machined Stainless Steel Sheet, Report MD/84/03, Materials Research Laboratories, Melbourne, Australia (1984).

TABLE 1

Composition of Parent Material (BS 95-15) and Weld Filler Material (BS 95-14)

Element	Parent Material BS 95-15	Parent Material Actual	Weld Filler Material BS 95-14	Weld Filler Material Actual
C	0.04/0.07	0.07	0.07 max	0.044
Mn	0.80/1.80	1.33	1.0 max	0.72
Si	0.7 max	0.36	0.7 max	0.41
S	0.025 max	0.006/0.008	0.025 max	0.004
P	0.035 max	0.020	0.035 max	0.019
Cr	15.3/16.3	15.86	13.2/14.7	14.2
Ni	5.2/6.0	5.47	5.0/6.0	5.35
Mo	1.2/2.0	1.78	1.2/2.0	1.50
Cu	1.4/2.1	1.77	1.2/2.0	1.75
Ti	0.05/0.15	0.09	-	-
Nb	-	0.05	0.2/0.5	0.24

Values are in weight percent.

TABLE 2

Mechanical Properties - Parent Material, Weld-Heat Treated, Repair Weld

Mechanical Property	Parent Material				Weld-HT		Repair Weld
	Aged 450°C		Aged 530°C		Aged 450°C	Aged 530°C	Not Aged
	BS 95-15	Actual (1)	BS 95-15	Actual (1)	Actual (2)	Actual (2)	Actual (3)
Yield Strength at 0.2% offset (MPa)	900 min	1138	800 min	993	1052	960	523
Tensile Strength (MPa)	1170/1360	1196	990/1170	1044	1174	1060	-
Elongation (%-50 mm G.L.)	6 min	15	8 min	19	-	-	-

(1) Test data from 4 mm round tensile specimens (av. of two)

(2) Test data from 3 mm thick rectangular tensile specimens (av. of two) - fracture in parent material

(3) Test data from 2 mm thick rectangular specimen (one specimen)

TABLE 3

Stress vs Number of Cycles to Failure (Crack Initiation) of Parent Material, Weld-Heat Treated, Repair Weld

Maximum Tensile Stress (MPa)	Parent Material Aged 530°C	No. of cycles to failure Weld-HT Aged 530°C	Weld-HT Aged 450°C	Repair Weld Not Aged
600	–	–	–	69,150
	–	–	–	121,890
	–	–	–	130,650
700	–	221,080	154,210	26,800
	–	286,250	397,960	34,360
	–	142,340	143,460	41,330
800	170,940	117,370	85,240	11,840
	199,730	126,360	118,340	13,900
	–	200,500	233,500	14,250
900	–	26,840	37,170	8,890
	–	43,960	43,850	11,470
	–	48,920	76,560	7,760

Notes: (1) R = 0.025, 5 Hz frequency

(2) All Weld-Heat Treated specimens failed in the parent material

(3) All Repair Weld specimens failed in the heat-affected zone

TABLE 4

da/dN vs ΔK for Parent Material - CT Specimens

Specimen	OLA	OLB	NLA	NLB	OTA	OTB	NTA	NTB
$C \times 10^{-15}$	37.2	71.1	32.6	6.77	50582	1380	2173	208
m	4.30	4.13	4.46	4.88	2.36	3.27	3.22	3.83
da/dN (m/cycle)	$55 \times 10^{-15}.\Delta K^{4.2}$		$14.4 \times 10^{-15}.\Delta K^{4.7}$		$6 \times 10^{-12}.\Delta K^{2.9}$		$6.1 \times 10^{-13}.\Delta K^{3.55}$	
r		0.96		0.95		0.97		0.97
B (mm)	5.954	5.944	5.937	5.959	5.953	5.944	5.941	5.947
W (mm)	50.998	51.022	50.945	51.084	51.949	50.977	50.998	50.981

Notes:

(1) $K = (\Delta P/B.W)\sqrt{a}.Y$ where Y is calculated from experimental compliance data on 13 mm thick MRL-CT specimens
$Y = 70.059 - 477.166\,X + 1411.66\,X^2 - 1839.88\,X^3 + 953.69\,X^4$ where $X = a/W$ $0.55 \leq x \leq 0.70$

(2) Specimen Designation:
- O – average ($530^{o}C$)
- N – normal age ($450^{o}C$)
- L – crack parallel to longitudinal (rolling) direction
- T – crack transverse to rolling direction
- A&B – two specimens each series

(3) PreCrack - Pmax = 7 kN, R = 0.1, 8 Hz frequency, sinusoidal waveform, room temperature
ΔK_{final} Range - 37.12 to 37.89 MPa $\sqrt{m}$,
Δa Range - 2.25 to 2.56 mm

(4) Test - Pmax = 6 kN, R = 0.1, 3 Hz frequency, sinusoidal waveform, room temperature
ΔK_{final} Range - 65.9 to 68.0 MPa $\sqrt{m}$

(5) $W-a > 4/\pi\ (K_{max}/\sigma_{ys})^2$ for all specimens

(6) Secant analysis method used for converting a-N data to da/dN

(7) Crack curvature resulted in less than 5% change in ΔK for all specimens

(8) Crack length measurement error - ± 0.025 mm

(9) Yield Strength - σ_{ys} for OL and OT = 993 MPa, σ_{ys} for NL and NT = 1138 MPa

TABLE 5

J_{Ic} Test Results for Parent Material - CT Specimens

Specimen	OLA	OLB	OTA	OTB	NLA	NLB	NTA	NTB
a_o/w (compliance)	0.601	0.609	0.602	0.604	0.611	0.607	0.604	0.608
a_o/w (measured)	0.614	0.621	0.603	0.615	0.623	0.619	0.618	0.623
Δa_f (mm) (compliance)	0.876	2.001	0.903	1.669	1.620	1.845	2.083	2.169
Δa_f (mm) (measured)	1.329	2.767	1.068	3.604	2.323	2.477	2.569	2.676
J_{Ic} (kN/m)	24.4	27.0	154.0	151.9	39.2	36.4	72.6	52.8
K_{Jc} (MPa $\sqrt{m}$)	69.0	72.6	173.3	172.1	87.4	84.2	119.0	101.5
$(E/\sigma_f^2)\,\Delta J/\Delta a_p$	19.4	20.4	32.2	32.2	6.5	6.8	19.0	15.6

Notes: (1) B (thickness) and b_1 (initial uncracked ligament) > $25/\sigma_y \cdot J_{Ic}$ & $15/\sigma_y \cdot J$ for all specimens

(2) $\Delta J/\Delta a_p < \sigma_f$ for all specimens

(3) $K_{Jc} = \sqrt{J_{Ic} \cdot E}$

(4) Compliance equation: $y = 0.1069 + 1.4755 \times 10^{-2} X - 1.6242 \times 10^{-4} X^2 + 8.7544 \times 10^{-7} X^3 - 1.7796 \times 10^{-9} X^4$ where $y = a/w$ and $X = EBV_{LL}/P$

(5) Measured values - average of eleven measurements equally spaced across the specimen - surface crack lengths given half the weight of interior measurements

(6) Max deviation of any single pre-crack length from average value was 3.5%.

(7) σ_f = 1018.5 MPa for Overage (O) specimens, σ_f = 1167 MPa for normal age (N) specimens: $\sigma_f = (\sigma_{ys} + \sigma_{ts})/2$

(8) $E = 195 \times 10^3$ MPa - from Tensile specimen tests

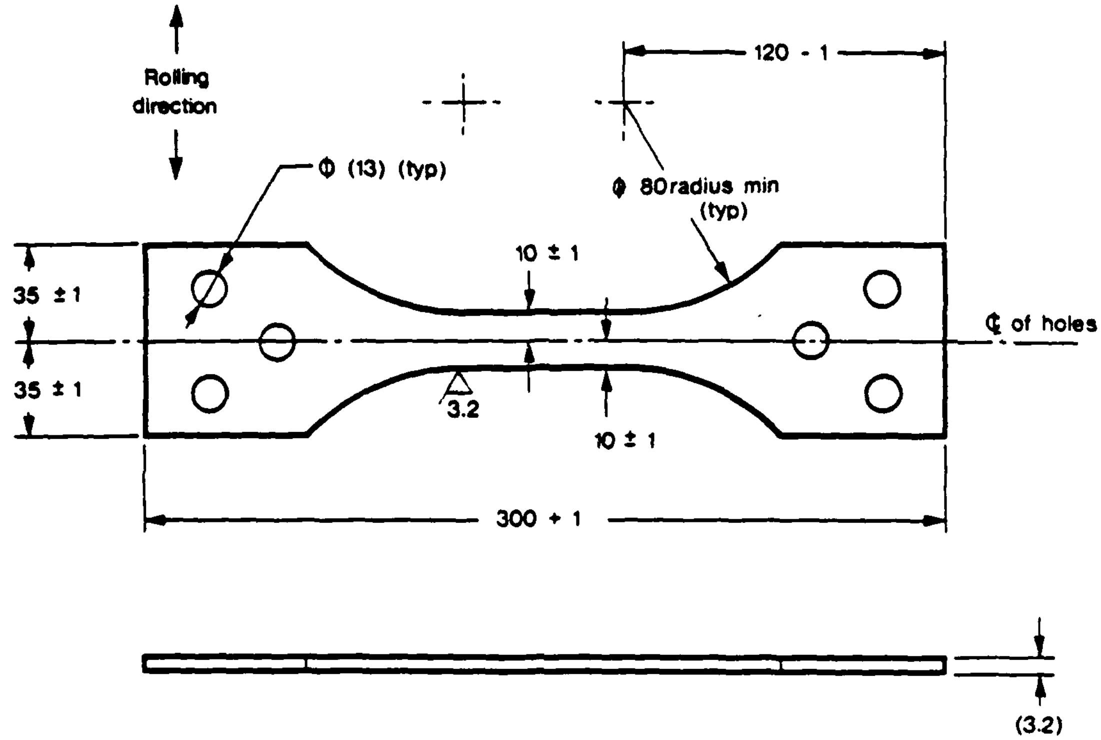

FIGURE 1a Geometry of original fatigue specimen.

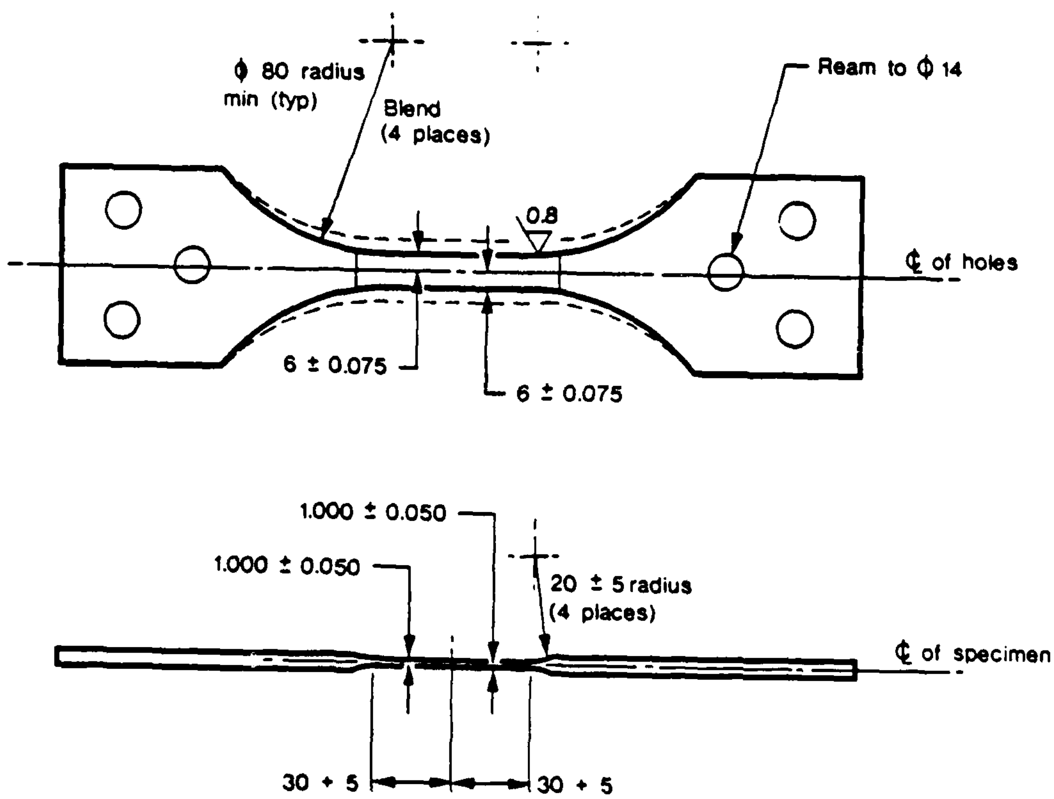

FIGURE 1b Geometry of final-modified fatigue specimen.

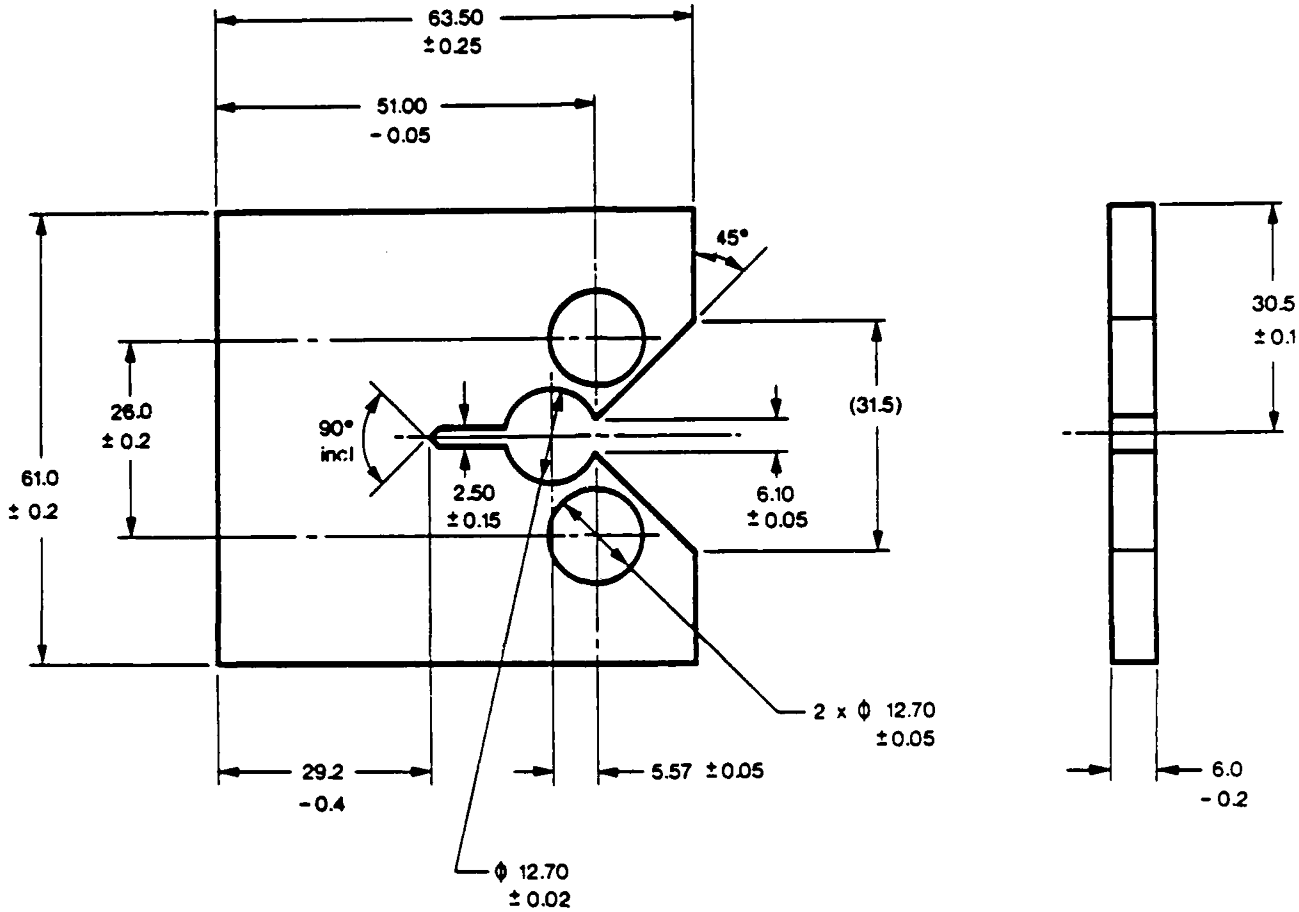

FIGURE 2 Geometry of CT specimen - MRL design.

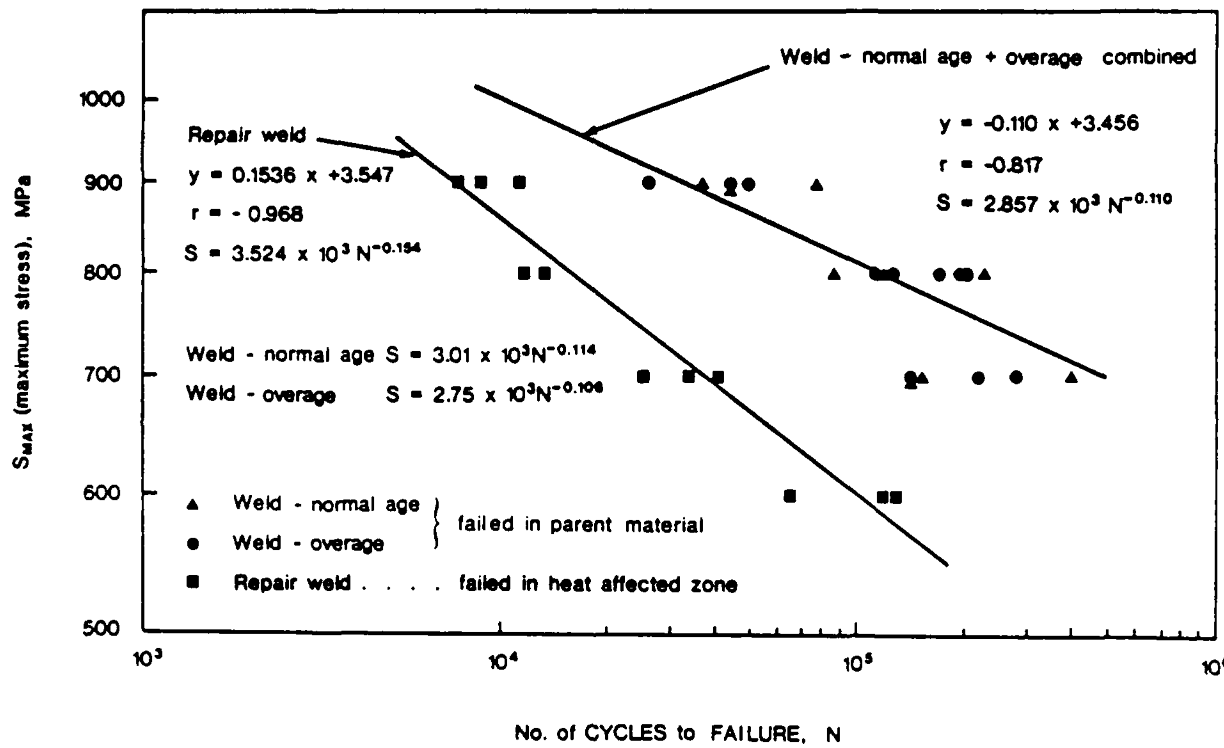

FIGURE 3 Stress vs number of cycles to failure-parent material and repair weld condition.

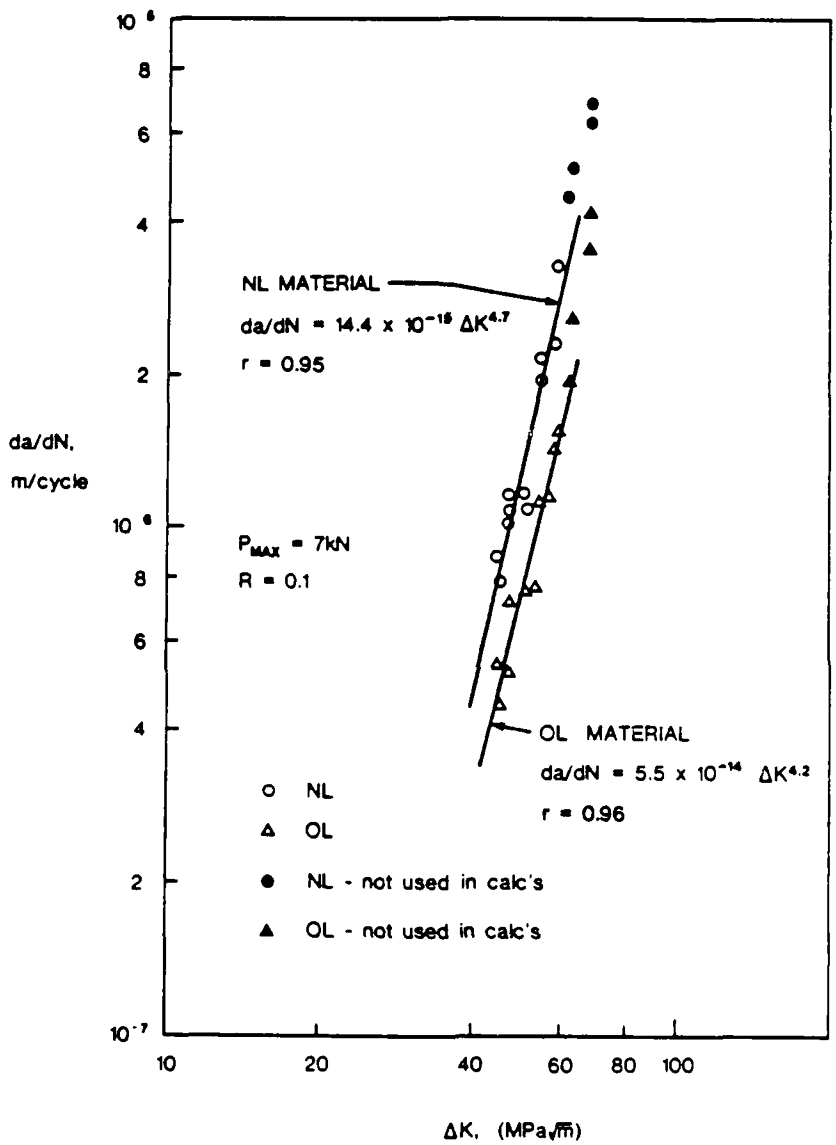

FIGURE 4 Fatigue crack growth rate results for material in the normal and overaged conditions, tested in the longitudinal direction.

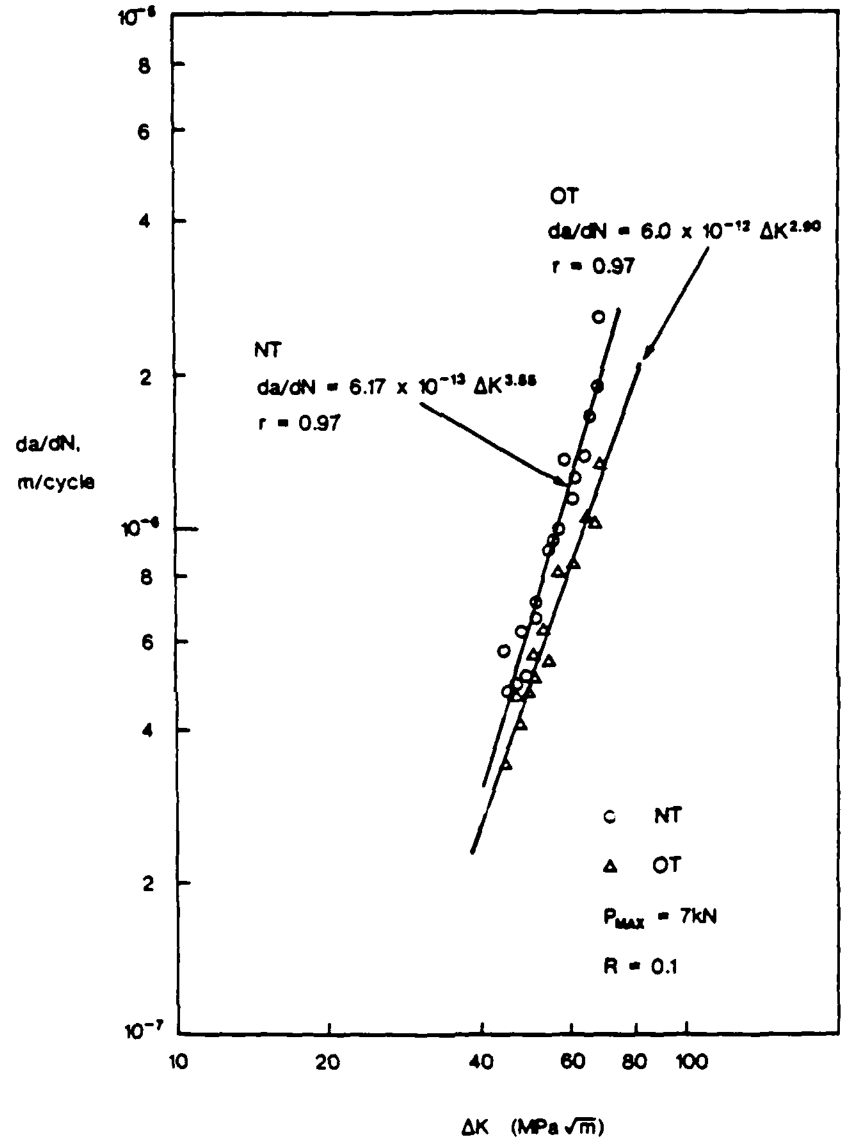

FIGURE 5 Fatigue crack growth rate results for material in the normal and overaged conditions, tested in the transverse direction.

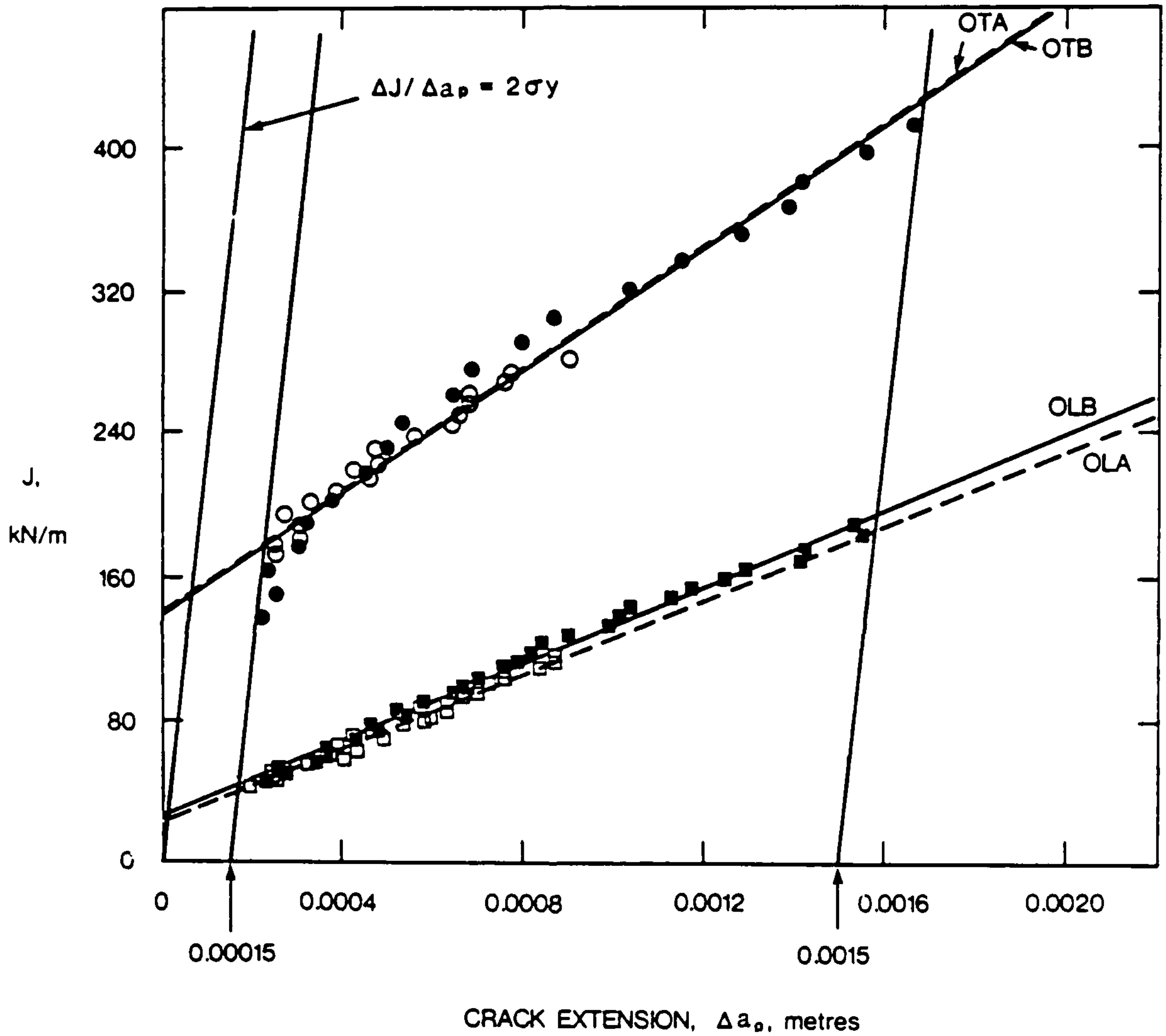

FIGURE 6 J vs Δa_p - STA 60 parent material, overaged, longitudinal and transverse directions.

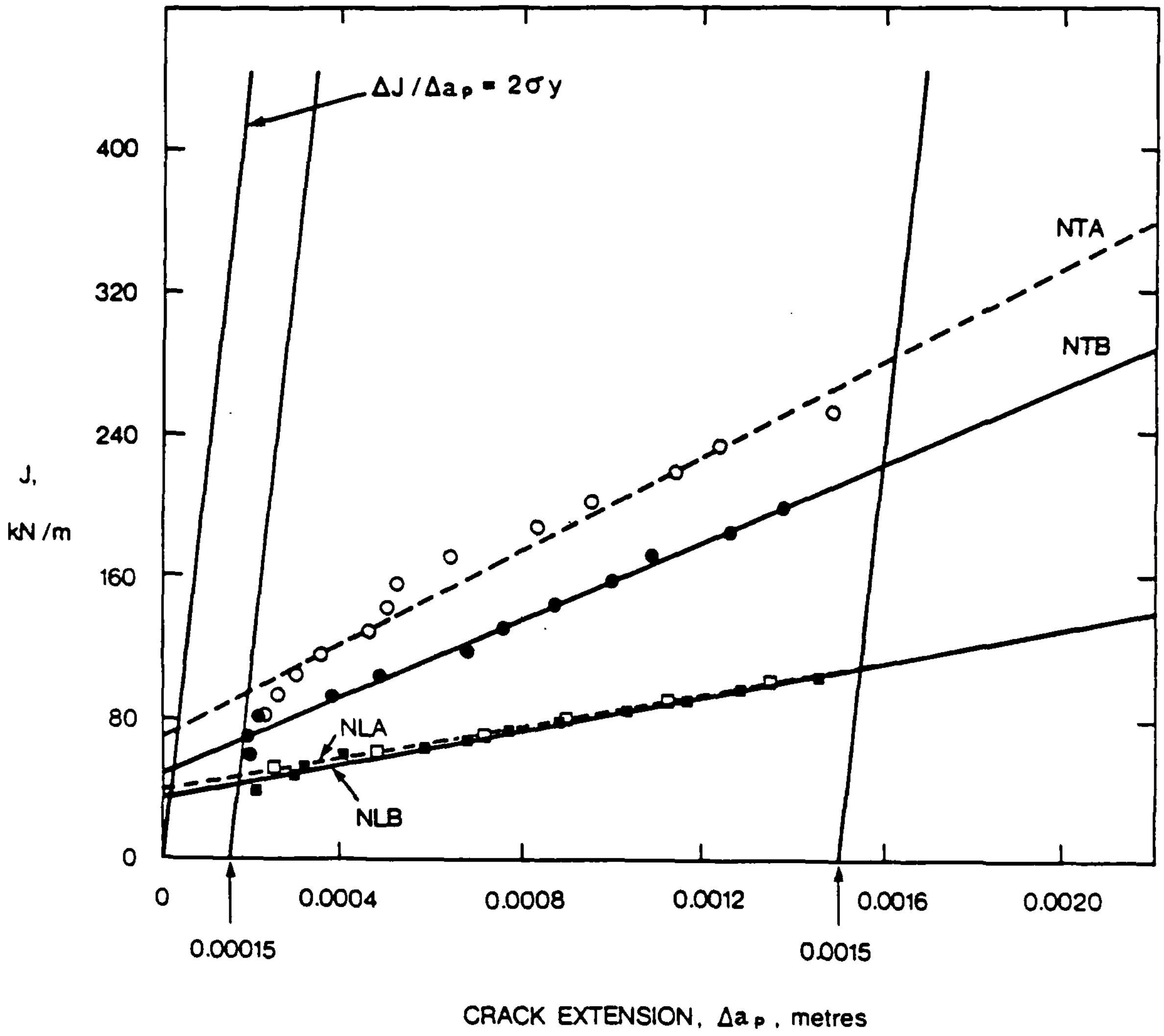

FIGURE 7 J vs Δa_p - STA 60 parent material, normal aged, longitudinal and transverse directions.

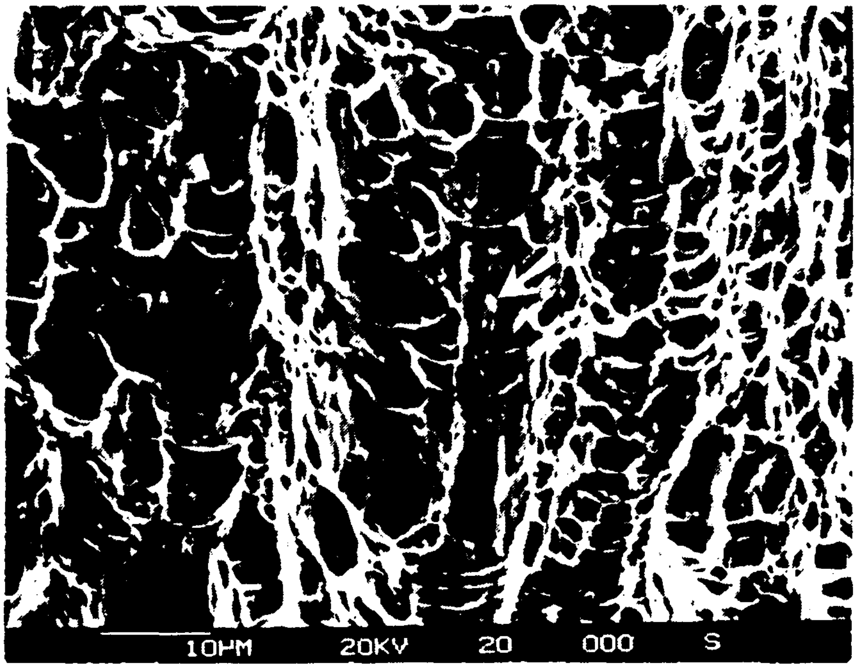

FIGURE 8 Manganese sulphide stringers in the STA 60 plate. Arrow points to a representative stringer. Scanning electron micrograph.

TECHNICAL REPORT INTERNAL DISTRIBUTION LIST

	NO. OF COPIES
CHIEF, DEVELOPMENT ENGINEERING BRANCH	
ATTN: SMCAR-CCB-D	1
-DA	1
-DC	1
-DM	1
-DP	1
-DR	1
-DS (SYSTEMS)	1
CHIEF, ENGINEERING SUPPORT BRANCH	
ATTN: SMCAR-CCB-S	1
-SE	1
CHIEF, RESEARCH BRANCH	
ATTN: SMCAR-CCB-R	2
-R (ELLEN FOGARTY)	1
-RA	1
-RM	1
-RP	1
-RT	1
TECHNICAL LIBRARY ATTN: SMCAR-CCB-TL	5
TECHNICAL PUBLICATIONS & EDITING UNIT ATTN: SMCAR-CCB-TL	2
DIRECTOR, OPERATIONS DIRECTORATE ATTN: SMCWV-OD	1
DIRECTOR, PROCUREMENT DIRECTORATE ATTN: SMCWV-PP	1
DIRECTOR, PRODUCT ASSURANCE DIRECTORATE ATTN: SMCWV-QA	1

NOTE: PLEASE NOTIFY DIRECTOR, BENET LABORATORIES, ATTN: SMCAR-CCB-TL, OF ANY ADDRESS CHANGES.

TECHNICAL REPORT EXTERNAL DISTRIBUTION LIST

	NO. OF COPIES
ASST SEC OF THE ARMY RESEARCH AND DEVELOPMENT ATTN: DEPT FOR SCI AND TECH THE PENTAGON WASHINGTON, D.C. 20310-0103	1
ADMINISTRATOR DEFENSE TECHNICAL INFO CENTER ATTN: DTIC-FDAC CAMERON STATION ALEXANDRIA, VA 22304-6145	12
COMMANDER US ARMY ARDEC ATTN: SMCAR-AEE	1
SMCAR-AES, BLDG. 321	1
SMCAR-AET-O, BLDG. 351N	1
SMCAR-CC	1
SMCAR-CCP-A	1
SMCAR-FSA	1
SMCAR-FSM-E	1
SMCAR-FSS-D, BLDG. 94	1
SMCAR-IMI-I (STINFO) BLDG. 59 PICATINNY ARSENAL, NJ 07806-5000	2
DIRECTOR US ARMY BALLISTIC RESEARCH LABORATORY ATTN: SLCBR-DD-T, BLDG. 305 ABERDEEN PROVING GROUND, MD 21005-5066	1
DIRECTOR US ARMY MATERIEL SYSTEMS ANALYSIS ACTV ATTN: AMXSY-MP ABERDEEN PROVING GROUND, MD 21005-5071	1
COMMANDER HQ, AMCCOM ATTN: AMSMC-IMP-L ROCK ISLAND, IL 61299-6000	1
COMMANDER ROCK ISLAND ARSENAL ATTN: SMCRI-ENM ROCK ISLAND, IL 61299-5000	1
DIRECTOR US ARMY INDUSTRIAL BASE ENGR ACTV ATTN: AMXIB-P ROCK ISLAND, IL 61299-7260	1
COMMANDER US ARMY TANK-AUTMV R&D COMMAND ATTN: AMSTA-DDL (TECH LIB) WARREN, MI 48397-5000	1
COMMANDER US MILITARY ACADEMY ATTN: DEPARTMENT OF MECHANICS WEST POINT, NY 10996-1792	1
US ARMY MISSILE COMMAND REDSTONE SCIENTIFIC INFO CTR ATTN: DOCUMENTS SECT, BLDG. 4484 REDSTONE ARSENAL, AL 35898-5241	2
COMMANDER US ARMY FGN SCIENCE AND TECH CTR ATTN: DRXST-SD 220 7TH STREET, N.E. CHARLOTTESVILLE, VA 22901	1
COMMANDER US ARMY LABCOM MATERIALS TECHNOLOGY LAB ATTN: SLCMT-IML (TECH LIB) WATERTOWN, MA 02172-0001	2

NOTE: PLEASE NOTIFY COMMANDER, ARMAMENT RESEARCH, DEVELOPMENT, AND ENGINEERING CENTER, US ARMY AMCCOM, ATTN: BENET LABORATORIES, SMCAR-CCB-TL, WATERVLIET, NY 12189-4050, OF ANY ADDRESS CHANGES.

TECHNICAL REPORT EXTERNAL DISTRIBUTION LIST (CONT'D)

	NO. OF COPIES
COMMANDER US ARMY LABCOM, ISA ATTN: SLCIS-IM-TL 2800 POWDER MILL ROAD ADELPHI, MD 20783-1145	1
COMMANDER US ARMY RESEARCH OFFICE ATTN: CHIEF, IPO P.O. BOX 12211 RESEARCH TRIANGLE PARK, NC 27709-2211	1
DIRECTOR US NAVAL RESEARCH LAB ATTN: MATERIALS SCI & TECH DIVISION	1
CODE 26-27 (DOC LIB) WASHINGTON, D.C. 20375	1
COMMANDER AIR FORCE ARMAMENT LABORATORY ATTN: AFATL/MN EGLIN AFB, FL 32542-5434	1
COMMANDER AIR FORCE ARMAMENT LABORATORY ATTN: AFATL/MNF EGLIN AFB, FL 32542-5434	1
METALS AND CERAMICS INFO CTR BATTELLE COLUMBUS DIVISION 505 KING AVENUE COLUMBUS, OH 43201-2693	1

NOTE: PLEASE NOTIFY COMMANDER, ARMAMENT RESEARCH, DEVELOPMENT, AND ENGINEERING CENTER, US ARMY AMCCOM, ATTN: BENET LABORATORIES, SMCAR-CCB-TL, WATERVLIET, NY 12189-4050, OF ANY ADDRESS CHANGES.